

Joseph Spencer

Mr. Taddiken, Mr. Miserendino

McMullen Capstone 903

6 January 2021

An Exploration of Path Tracking on a Small Nonholonomic Robot

An Exploration of Path Tracking on a Small Nonholonomic Robot

Joseph Spencer



Mr. Miserendino and Mr. Taddiken

McMullen Capstone Experience

6 January 2021

CONTENTS

1	Introduction	4
2	Test Vehicle	6
2.1	Physical Specifications	6
2.2	Control Architecture	8
2.3	Position Tracking / Odometry	12
3	Path Tracking Algorithms	14
3.1	Follow-The-Carrot	14
3.2	Pure Pursuit	16
3.2.1	Adaptive Lookahead Distance with Respect to Lateral Error	17
3.2.2	Adaptive Lookahead Distance with Respect to Curvature	18
3.3	The Stanley Method	19
3.4	Follow the Past	21
3.5	Vector Pursuit	23
3.6	Ramsete	27
4	Testing Results	28
4.1	Paths and Errors	28
4.2	Follow The Carrot	30
4.3	Pure Pursuit	32
4.4	Pure Pursuit Adaptive - Lateral Error	34
4.5	Pure Pursuit Adaptive - Curvature	36
4.6	Stanley Method	38

4.7	Follow The Past	40
4.8	Vector Pursuit	42
4.9	Ramsete	44
4.10	Further Data	46
5	Conclusion	46

Abstract

Path tracking is a specific problem within the field of controls engineering that seeks to devise methods of following a path with an autonomous robot. There are many variations of path tracking that have been designed for different vehicles. This paper will give an overview of the process of path tracking and explore various algorithms used for path tracking, as well as some variations using adaptable parameters. Thereafter, the algorithms and their variations will be tested using a small skid-steer robotic vehicle constructed from VEX Robotics parts. Telemetry data from these tests is used to assess each algorithm's performance, and this data is analyzed to suggest future improvements. Results indicate good performance from staple path tracking algorithms like Pure Pursuit and Follow the Carrot, suggest potential for algorithms like Ramsete to be used for path tracking, as well as demonstrate efficacy in adaptive modifications to such algorithms.

1. INTRODUCTION

Path tracking is one of the most common methods of controlling complex movement of autonomous vehicles and robots. Recent history has shown great strides in self-driving cars, such as the DARPA Grand and Urban Challenges in 2004/2005 and 2006 respectively, and the diversity of path tracking algorithms continues to grow. Given that path tracking only needs information of the path segments immediately in front of it, it is highly flexible and useful in applications where the path is being generated in real-time. Alternatives, such as motion profiling, usually need full knowledge of a motion before execution.

Path tracking uses an arbitrary path to govern an autonomous vehicle's motion from point A to point B. This is nontrivial as a result of the robot existing in three degrees of freedom, position on a two-dimensional surface and a heading about that surface. Most robots have only two controls to navigate these degrees of freedom: velocity and steering in an Ackerman, or car-like, steering mechanism, or left-side velocity and right-side velocity in a skid-steer or tank-like drive. This property of having less degrees of control than freedom is known as being nonholonomic. Certain other types of drive trains, such as mecanum or Kiwi drives do not have this constraint, allowing them to additionally move laterally, and are therefore called holonomic drives. This additional degree of control allows them to move in all directions regardless of heading, which makes path tracking less useful, as a better solution is usually to move in a straight line from one point to another.

Most path tracking algorithms must be tuned, meaning they have some set of constant variables which dictates the behavior of the algorithm. In many cases, these values present a tradeoff of aggression and smoothness. A more aggressive tuning will make a greater effort to be on the path, while a smoother tuning may stray from the path more easily but complete the path

more quickly due to its less jerky motion. Having both a smooth path and accurate tracking with minimal error is the ideal of path tracking.

Path tracking as a whole is a system of four parts: path generation, point finding, the tracking algorithm, and motor control. Path generation consists of the creation of a function, normally a parameterized piecewise interpolation function that connects the desired start and end points, and sometimes additional points between the two. The data of the path can be stored as a predetermined set of waypoints on the path, or as a function, which the robot will be able to sample to find points. More advanced systems, such as a self-driving car, could create the path in real-time. Using cameras, radar, and other sensors, a self-driving car could set the path waypoints just ahead of the vehicle while the vehicle travels.

After this, while the vehicle is attempting to follow the path, it must find and select a point on the path. The exact properties of this point are dependent on what data is necessary for the next step; however, most algorithms use a goal or lookahead point. A goal point is usually defined as a point that is both on the path and on a circle of a set radius around the vehicle. By setting this radius equal to the lookahead distance, this sets the goal point such that it is one lookahead distance ahead of the vehicle. This lookahead distance becomes a value that is tuned, either by a preset constant or function of something in the environment, in order to maximize controller performance. Lookahead distance is usually tuned by trial-and-error, following the general rule that a larger lookahead distance is more stable, creating less jerky motion, while a smaller lookahead distance follows the path more tightly. However, some tracking algorithms utilize the point on the path nearest to the robot instead, so no lookahead distance is needed. Implicit to this system is the need for the robot to know its own position. This can be done using a position tracking system such as GPS or odometry. GPS uses satellite triangulation to estimate the position of a GPS receiver, while odometry is a type of position tracking which uses a variety

of sensors such as shaft encoders and inertial measurement units (IMUs) to integrate changes in sensor data to iteratively estimate position.

Thereafter, the tracking algorithm is applied, which takes the information of the robot's position and the previously selected point and determines a desired instantaneous motion. The form of this desired instantaneous motion varies between algorithms, as some algorithms designed for Ackerman steering will give a desired speed and turning angle, while others designed for skid-steer drives give a desired speed and instantaneous curvature of the vehicle's motion.

Finally, the desired instantaneous motion must be executed by the motors. There exist countless ways to do this, from simple modified-PID controllers to advanced systems using machine learning. All of these systems attempt to keep the measured velocity equal to the desired, or reference, velocity. Due to the sheer number and complication of many control methods, this topic will not be discussed generally here. The Capstone research encompasses a diverse set of path tracking algorithms as well as test their efficacy when applied to the test vehicle. By developing a calculable way to measure deviancy from the path, the algorithms can be empirically tested and reviewed as well as reveal possible improvements to the algorithms.

2. TEST VEHICLE

For the purposes of testing the path tracking algorithms explained hereafter, a small robot has been built using parts standard to the VEX Robotics v5 system. It does not have any mechanisms besides the drive train, as it is designed specifically for drive train testing.

2.1. PHYSICAL SPECIFICATIONS

The robot is an eight wheeled vehicle, four of which are larger powered wheels and four of which are smaller tracking wheels. The radius of the larger wheels is approximately 5.24 cm (2.06 in) and the radius of the smaller wheels is approximately 3.49 cm (1.38 in). The powered

wheels are each independently driven by one VEX v5 motor with an 18:1 gearbox, providing about 220 rpm with a stall torque of 1 Nm. Each of the tracking wheels are connected to an optical shaft encoder, reading 360 ticks per rotation. These tracking wheels are used for the position tracking of the robot and are separate from the powered wheels to avoid sensor noise in the form of wheel slippage, which may occur when the vehicle accelerates. The structural chassis of the robot measures $44.45\text{ cm} \times 44.45\text{ cm} \times 10.48\text{ cm}$ (17.5 in \times 17.5 in \times 4.13 in), while the powered wheels have a chassis width of 37.62 cm (14.81 in). The tracking wheels in line with the powered wheels are 33.81 cm (13.31 in) apart and the tracking wheels perpendicular to the powered wheels are 27.64 cm (10.88 in) apart. The rear powered wheels have screws put into the rollers, which drastically increases the lateral static friction of those wheels. Without this modification, going around a turn would result in an amount of lateral velocity that is unmanageable for the tracking algorithms, resulting in poor performance for all algorithms.

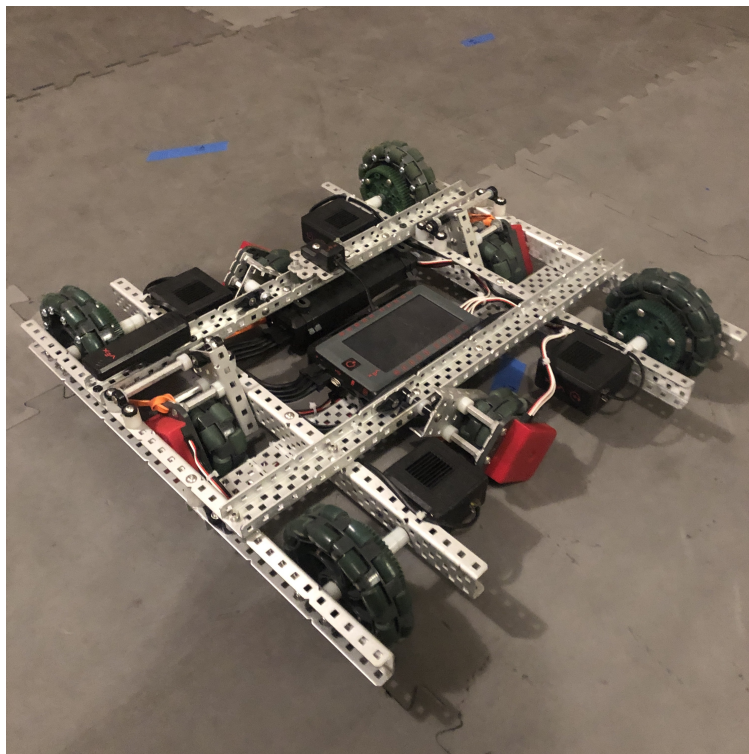


Fig. 1. The Test Vehicle

The vehicle is designed to have a wide platform which maximizes the control and sensitivity to rotational change, as measuring a rotation far from the center maximizes angular resolution. In addition to the tracking wheels, the vehicle is also equipped with an IMU, which is used to mitigate accumulating error in the estimated heading, and a radio, for wireless communication with a controller.

2.2. CONTROL ARCHITECTURE

The vehicle is programmed in C++ using the PROS kernel, alongside KappaFramework to organize the control architecture. Additionally, the path generation is pregenerated using a python script. The standard path generation will be a cubic Hermite spline, or a piecewise set of cubic Hermite curves. Cubic Hermite curves take the desired position and first derivative with respect to parameter t of both x and y , at both $t = 0$ and $t = 1$ to produce a parametric function on $t \in [0, 1]$. The derivations of Wagner et al. for Hermite curves are:

$$x(t) = (2t^3 - 3t^2 + 1)x(0) + (-2t^3 + 3t^2)x(1) + (t^3 - 2t^2 + t)x'(0) + (t^3 - t^2)x'(1) \quad (1a)$$

$$y(t) = (2t^3 - 3t^2 + 1)y(0) + (-2t^3 + 3t^2)y(1) + (t^3 - 2t^2 + t)y'(0) + (t^3 - t^2)y'(1) \quad (1b)$$

for any desired behaviors of the function.

In order to store the path information, the functions will be sampled for points on the path. Points will be chosen such that they are spaced about 5 cm apart and saved as binary data accessible to the vehicle. Three different paths, two of which are random shapes, as well as a figure-8, will be used in algorithm testing; these paths will be shown in the analysis of the telemetry collected during testing.

As the vehicle follows the path, it will select points iteratively, stepping through the binary data as it passes the corresponding points. For the selection of a lookahead point, the nearest waypoint outside of the lookahead distance will be found, and a line segment will be generated

between it and the previous waypoint. The lookahead point will be selected as the point on the line segment that is exactly the lookahead distance away from the robot. A similar interpolation mechanism is used by Sidhu et al., who claim that without interpolation “the resulting steering command ... becomes jerky unless the path points are quite close together” (4). Placing path waypoints closer together requires a greater amount of computation time to find a point and is therefore not desirable.

The path tracking implementations will be the changing variable in the experimentation, in order to assess their efficacy. Given the diversity in path tracking algorithms, they can give their control output in many different forms, so a conversion to a standardized control output must be used. This standardized output will be in the form of (v, ω) , desired forward speed and desired counterclockwise angular velocity. Firstly, instantaneous curvature γ can be converted to angular velocity by the following:

$$\gamma = \frac{d\theta}{ds} \quad (2a)$$

$$\gamma \cdot \frac{ds}{dt} = \frac{d\theta}{ds} \cdot \frac{ds}{dt} \quad (2b)$$

$$\gamma \cdot v = \omega \quad (2c)$$

Note that the faster the vehicle is moving, the more aggressively the vehicle will react to a desired curvature.

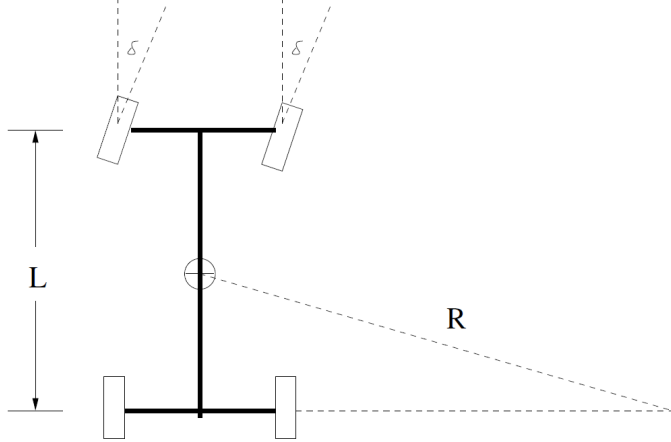


Fig. 2. Diagram of an Ackerman drive (Giesbrecht et al. 13)

In addition to curvature, some algorithms designed for Ackerman steering (fig. 2) give a control output in the form of turning angle; essentially, what degree the front wheels of the vehicle are turned relative to the tangential motion of the vehicle. This angle is commonly denoted as δ . By calculating the curvature γ of the circle created by turning angle δ , the following is yielded:

$$\gamma = \frac{1}{l} \tan(\delta) \quad (3)$$

where l is the distance between the actuation point of the front wheel and the rear axle. For the purposes of this paper, this will be considered a tuning variable. Applying equation 2c yields:

$$\omega = \frac{v}{l} \tan(\delta) \quad (4)$$

Equations 2c and 4 will be used frequently hereafter to convert control signals into something that can be handled by a skid-steer vehicle.

Additionally, many path tracking algorithms do not specify a desired speed, only a turning command. In this case, a constant desired speed of 100 cm/s (182 rpm) will be used. After being provided with a desired speed v and angular velocity ω in rad/s, the robot converts this to

a desired angular velocity in rpm for the left ω_l and right ω_r sides of the drive train using:

$$\omega_l = \frac{30 \cdot v - 15 \cdot \omega \cdot d}{\pi \cdot r} \quad (5a)$$

$$\omega_r = \frac{30 \cdot v + 15 \cdot \omega \cdot d}{\pi \cdot r} \quad (5b)$$

for wheel radius r and chassis width d . The unit change here is simply because it is easier to calculate angular velocity in rad/s in the context of moving through a plane, while rpm is more intuitive for a spinning wheel.

These targets are then given to a modified velocity PD controller of the form:

$$e_j(t) = \omega_j - \omega_{j_a} \quad (6a)$$

$$u_j(t) = k_f \cdot \omega_j + k_{sf} \cdot \text{sgn}(\omega_j) + \int_0^t k_p \cdot e_j(\tau) + k_d \frac{de_j(\tau)}{d\tau} d\tau \quad (6b)$$

for a j corresponding to either l or r for either side of the vehicle, ω_{j_a} corresponding to the measured angular velocity on side j , all of the k values being tunable constants, $u_j(t)$ being the voltage sent to the motor in mV, bounded between ± 12000 , and $\text{sgn}()$ being the sign function. The idea of this controller is taken from OkapiLib, a library used widely with VEX robots such as this test vehicle.

The first two terms are feedforward, indifferent to the measured error, and are intended to estimate the voltage needed to spin at the desired velocity. The first scales linearly with the desired speed, while the second is a constant voltage in the direction of the desired motion, ensuring the static friction is overcome regardless of the target speed. The latter two terms in the integral are feedback, responding to the measured error to bring the angular velocity to the target velocity if the feedforward terms are insufficient. The first of these terms is proportional to the error, driving it to zero, while the other attempts to bring the derivative of the error with respect to time to zero, dampening any oscillations that may appear. These terms are then integrated, as

an increasing control effort is necessary to accelerate to the target velocity. Unlike controlling position, a constant voltage does not significantly change velocity. Additionally, this integral is bounded such that its value may not exceed some bounds, usually the voltage constraints of the motor. This allows the integral value to immediately start changing the voltage of the motor should the sign of the error change.

The controller for this vehicle was tuned by first measuring the minimum voltage needed to overcome static friction, for k_{sf} , as well as calculating the slope between $(k_{sf}, 0)$ and (u_{max}, ω_{max}) for k_f . The feedback terms were then found by trial and error. The tuning used with this vehicle is:

$$k_f = 50 \quad k_{sf} = 620 \quad k_p = 60 \quad k_d = 50$$

2.3. POSITION TRACKING / ODOMETRY

In addition to the aforementioned control structure, a position tracking system is needed to track the position of the vehicle. The position of the vehicle must be monitored in order to determine which goal points should be selected, as well as to convert that goal point into the local coordinate system of the vehicle for analysis by the path tracking algorithm. It is also a requirement for measuring the efficacy of the path tracking algorithms, as any function which measures the vehicle's deviance from the path must know the vehicle's position relative thereto.

Multiple implementations of odometry were considered for use, all of which were modifications of either the method described by Crowley or VRC Team 5225. Crowley's implementation estimates the displacement forwards ΔD and the change in heading $\Delta\theta$ using a two tracking wheel system, both of which face tangentially to the vehicle's heading. These equations are shown as the following:

$$\Delta D = \frac{\Delta R + \Delta L}{2} \tag{7a}$$

$$\Delta\theta = \frac{\Delta R - \Delta L}{w} \quad (7b)$$

in which R and L track accumulated arclength tangential to the vehicle's heading on the right and left sides with w being the distance between them. These arclengths are commonly monitored by tracking wheels, such as those shown on the test vehicle in fig. 1.

Team 5225's method differs in two ways; namely, a more precise estimation of displacement and a consideration for lateral displacement. By assuming the curvature over the iteration interval is constant, a circle can be used to estimate the vehicle's motion. In this case, the displacement is given by a chord of the circle. The displacement forwards ΔD and the change in heading $\Delta\theta$ are given by:

$$\Delta D_f = 2 \sin\left(\frac{\Delta\theta}{2}\right) \cdot \left(\frac{\Delta R}{\Delta\theta} + \frac{w}{2}\right) \quad (8a)$$

$$\Delta\theta = \frac{\Delta D_r - \Delta D_l}{w} \quad (8b)$$

Equation 8a can be rewritten as:

$$\Delta D_f = 2 \sin\left(\frac{\Delta\theta}{2}\right) \cdot \left(\frac{\Delta R + \Delta L}{2\Delta\theta}\right) \quad (8c)$$

$$\Delta D_f = \frac{2}{\Delta\theta} \sin\left(\frac{\Delta\theta}{2}\right) \cdot \left(\frac{\Delta R + \Delta L}{2}\right) \quad (8d)$$

$$\text{Note that: } \lim_{\Delta\theta \rightarrow 0} \Delta D_f = \frac{2}{\Delta\theta} \cdot \frac{\Delta\theta}{2} \cdot \left(\frac{\Delta R + \Delta L}{2}\right) \quad (8e)$$

$$\lim_{\Delta\theta \rightarrow 0} \Delta D_f = \left(\frac{\Delta R + \Delta L}{2}\right) \quad (8f)$$

therefore, for a sufficiently small $\Delta\theta$, the two methods are equivalent. This was verified in testing, in which the best performing variation of both types of implementation performed extremely similarly.

Both methods' implementations were found to perform best when modified to use an IMU, instead of encoders to track heading. The two tracking wheels facing each direction were used in accordance to each method's displacement estimation in not only the direction

tangential to the vehicle's heading, but also laterally. As stated previously, both method's best implementations performed very similarly. For this reason, as well as the modified Crowley method being computationally simpler than the Team 5225 method, the modified Crowley method was chosen for testing.

3. PATH TRACKING ALGORITHMS

3.1. FOLLOW-THE-CARROT

Follow-the-Carrot is one of the simplest forms of path tracking. It provides no control over the linear velocity of the vehicle and seeks only to make the robot face a selected point along the path, called the goal point or carrot point. It functions with the idea that facing a point on the path ahead of the vehicle while driving forward will keep the vehicle aligned and sufficiently close to the path; however, in implementation, this closeness is known to vary widely, and large lateral errors can be common in some paths.

This method first selects the carrot or goal point in accordance to a predefined lookahead distance from the vehicle. Using this point and the position of the vehicle, the target heading is calculated as the heading of the line pointing from the vehicle to the carrot point. The error e_0 can then be calculated as the difference between the target heading and the actual heading:

$$e_0 = \text{atan2}(y_2 - y_1, x_2 - x_1) - \theta \quad (9)$$

in which the point (x_1, y_1) is the position of the vehicle, θ is the vehicle's heading, and the point (x_2, y_2) is the carrot point.

This error then governs the angular velocity of the vehicle, causing it to turn towards the target heading. This can be done in two ways, either through a proportional gain (Lundgren) or a full PID controller (Hogg et al.). In the former method, the error is simply multiplied by a scalar

k_p , called the proportional gain, then assigned to the desired angular velocity of the vehicle ω :

$$\omega = k_p \cdot e_0 \quad (10)$$

However, to improve the performance of this controller, one can use a PID controller. A PID controller, instead of only considering the error at the current moment of time, considers the error itself (P), as well as the integral (I) and derivative (D) of the error with respect to time. It follows that each of these terms has its own gain value, k_p , k_i , and k_d respectively, to form the following equation:

$$\omega = k_p e_0 + k_i \int_0^t e_0(\tau) d\tau + k_d \frac{de_0(t)}{dt} \quad (11)$$

Using a PID controller instead of only a proportional term can add additional stability to the system, creating smoother motion which is able to reach the target more quickly. The integral term works to remove steady state error, or small errors that do not reduce to zero over time, usually caused by the motors not operating under a certain voltage. The derivative term prevents overshoot by dampening the system, which it does by applying a control signal in the opposite direction that the error is changing. While slightly counterintuitive, this causes the system to decelerate as it nears the target, ideally reaching the target with a speed of zero. Both additional control values usually make the system converge to the target more easily.

However, both versions of the Follow-the-Carrot algorithm are not necessarily effective. Lundgren notes that “the vehicle has a tendency to naturally cut corners” (3). This is because as the vehicle approaches a turn, as soon as the selected carrot point is within the turn, the vehicle will attempt to turn towards it, sometimes before the vehicle itself has reached the turn. Lundgren also claims that the vehicle could oscillate over the path. While the testing of Hogg et al. showed this effect to be minimal when using the PID method, it is likely a significant issue for the proportional-only method. This is likely because the lack of a derivative term means

there is no dampening on the system besides friction, which may be not be enough for a robot of sufficient mass.

3.2. PURE PURSUIT

The Pure Pursuit algorithm is one of the oldest and most popular algorithms in the field of path tracking, known for its robustness. It was first introduced into the field of path tracking in Dr. Wallace's "First Results in Robot Road-Following" and later popularized in Dr. Coulter's "Implementation of the Pure Pursuit Path Tracking Algorithm."

Pure Pursuit follows a similar procedure to Follow-the-Carrot in its goal point selection, choosing a point on the path that is a specified distance from the vehicle. However, rather than an error function and gains approach, Pure Pursuit uses a geometric system. Once a goal point has been determined, a circle is found that passes through both the position of the vehicle and the goal point, as well as being tangent to the heading of the vehicle (see fig. 3). This circle, therefore, describes a path from the current position of the robot to the goal point which requires the robot to drive with a constant curvature. This curvature becomes the control output from the algorithm.

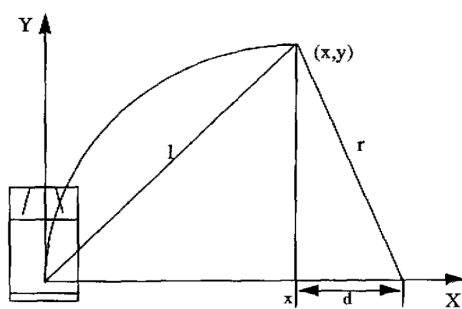


Fig. 3. Geometry of Pure Pursuit Algorithm (Coulter 5)

Note that in fig. 3, the point (x, y) corresponds to the goal point in the local coordinates

of the vehicle. The curvature of the circle γ , as derived by Coulter, can be calculated as follows:

$$d = r - x \quad (12a)$$

$$(r - x)^2 + y^2 = r^2 \quad (12b)$$

$$r^2 - 2rx + x^2 + y^2 = r^2 \quad (12c)$$

$$2rx = l^2 \quad (12d)$$

$$r = \frac{l^2}{2x} \quad (12e)$$

$$\gamma = \frac{2x}{l^2} \quad (12f)$$

Then, by equation 2c, the angular velocity is:

$$\omega = \frac{2x \cdot v}{l^2} \quad (13)$$

Additionally, note that the only parameter that can be tuned is the lookahead distance for the goal point. As an added benefit to the algorithm, this makes it much easier to tune than other algorithms with many tuning parameters. However, some variants of Pure Pursuit seek to increase performance by using a functionally defined lookahead distance, one that changes with respect to some measured value.

3.2.1. ADAPTIVE LOOKAHEAD DISTANCE WITH RESPECT TO LATERAL ERROR

One such method is described in Giesbrech et al.'s implementation of Pure Pursuit on a Raptor UGV. In this implementation, they directly add the lateral error between the path and the vehicle to the standard lookahead distance to produce the adaptive lookahead distance. This lateral error is calculated as the minimum distance between the vehicle and the line segment connecting the previous and next waypoints on the path. For a previous waypoint n , the next waypoint m , and the vehicle at point p , this calculation is:

$$\text{let } \vec{w} = p - n \quad (14a)$$

$$\text{let } \vec{v} = m - n \quad (14\text{b})$$

$$\text{let } b = n + \text{proj}_{\vec{v}} \vec{w} \quad (14\text{c})$$

$$L_{err} = ||p - b|| \quad (14\text{d})$$

$$L_{adapt} = L + L_{err} \quad (14\text{e})$$

in which L is the standard lookahead distance, and minimum value for the lookahead.

By doing this, two issues with the standard Pure Pursuit implementation are fixed. Firstly, as the effective lookahead distance is always greater than the lateral error, the path is necessarily within the lookahead distance of the vehicle. This means there will always be a valid goal point and there is not a need to handle the edge-case of straying from the path. Secondly, as stated by Giesbrecht et al., “by comparison with the non-adaptive lookahead results...the resultant trajectory can be made much smoother without sacrificing tracking accuracy” (14). A smoother trajectory means better performance, as jerky motion tends to slow down the vehicle; however, this usually comes at the cost of a maintained error with the path.

3.2.2. ADAPTIVE LOOKAHEAD DISTANCE WITH RESPECT TO CURVATURE

Another method of varying the lookahead distance is to adapt with respect to the path, rather than the vehicle’s performance. A similar kind of adaptive lookahead is seen in CF-Pursuit from Shan et al., which is another form of path tracking. One of the improvement their novel path tracking algorithms makes over Pure Pursuit is the use of a changing lookahead distance with respect to the curvature of the path over some domain ahead of the vehicle. While the specifics of CF-Pursuit will not be discussed, this trait can be applied as a variant to the Pure Pursuit algorithm. This curvature ahead of the vehicle γ can be approximated by:

$$\gamma = \frac{\Delta\theta}{\Delta s}$$

for an arbitrary, non-infinitesimal arclength Δs . For a path defined by a set of equally or approximately equally spaced waypoints indexed by i , this can be rewritten as

$$\gamma_i = \frac{\theta_{i+n} - \theta_i}{n \cdot \Delta s} \quad (15)$$

for a number of waypoints ahead n and a waypoint spacing of Δs .

As the curvature of the path increases, the ideal lookahead distance is smaller, as the larger the lookahead distance, the sooner a vehicle will attempt to cut a corner. Therefore, a suitable lookahead function is:

$$L_{adapt} = \frac{L}{1 + |\gamma| \cdot L} \quad (16)$$

for a base lookahead distance of L . This results in an effective lookahead distance of L for a straight path, setting L as the definitive upper bound for the effective lookahead distance. As γ increases, the effective lookahead distance decreases, which may improve tracking accuracy around corners. This function also remains dimensionally consistent as $|\gamma| \cdot L$ is unitless.

Shan et al. criticize their use of a curvature dependent lookahead distance; however, their method differs from the one described here. Significantly, the method used by Shan et al. to determining the lookahead distance was a fuzzy controller, which sampled curvature over multiple distances. Such an implementation may have been an over-complicated system that caused instability.

3.3. THE STANLEY METHOD

The Stanley Method of path tracking was developed by the Stanford Racing Team's entry in the 2005 DARPA Grand Challenge, an offroad autonomous automotive race. Given the offroad nature of the conditions this vehicle was expected to face, the algorithm has proved robust, especially following large disturbances. The Stanford Racing Team claimed the algorithm was able to produce results of "a typical root mean square (RMS) crosstrack error of under 0.1 m"

(Hoffmann et al. 1). Crosstrack here refers to the distance between the path and the vehicle, so a low value of crosstrack error corresponds to a close and accurate tracking of the path.

Unlike the previous methods, the Stanley Method does not use a lookahead distance, and instead looks at the point closest to the robot. While the authors do not specify how this point is found, one such implementation would be the one showed in equation 14c, which finds the nearest point b on the line between two waypoints. The primary motivation for doing this is to put a significant part of the controller's effort into aligning itself with the path. From this nearest point, it uses the heading of the point or tangent direction of the path at the point, the distance from the point to the vehicle's position, as well as the vehicle's velocity to determine the controller output. As a standard car was used as the original vehicle, the output of the controller is the angle to which the wheels are turned in the Ackerman steering mechanism. Additionally, factors such as a dampening gain for the inertia of the wheels' steering direction turning have been removed for the purposes of this paper, as they are not relevant to the skid-steer drive of the test vehicle. The original control law is as follows:

$$\delta(t) = \Psi(t) + \arctan \frac{k \cdot e(t)}{v(t)} \quad (17)$$

where δ is the steering angle, Ψ is the difference between the vehicle's heading and the nearest point's heading, k is a gain, e is the crosstrack error, and v is the velocity. The steering angle can then be converted to angular velocity by equation 4:

$$\omega(t) = \frac{v(t)}{l} \tan \left(\Psi(t) + \arctan \frac{k \cdot e(t)}{v(t)} \right) \quad (18)$$

in which l represents the distance between the front and rear wheels of Ackerman steering type vehicle that the skid-steer robot using this algorithm will be emulating. In this context, it will be considered a tuning variable.

The findings of the authors and outside sources reflect well on this algorithm. Hoffmann

et al. explain that the algorithm is mathematically proven to cause the vehicle to converge to the path exponentially, suggesting a high degree of robustness (4). Snider states that the Stanley method “is well suited for higher speed driving,” and it “outperforms Pure Pursuit in most scenarios” (17, 66). Pendleton et al. claim that “Compared to the pure pursuit method, the Stanley method, has better tracking results and does not cut corners” (30). They attribute this to the use of crosstrack error as opposed to a point pursuit. However, Pendleton et al. also state that the Stanley method may behave similarly to a Pure Pursuit controller with a small lookahead distance; namely, it oscillates over the path (31). This behavior is undesirable, as causes the vehicle to make excessive motions that both decelerate the vehicle and give the path planner less control over the vehicle’s motion, which could be potentially dangerous to the vehicle or the surrounding environment. Regardless, the Stanford Racing Team used the Stanley method to record the fastest completion time in the DARPA Grand Challenge 2005.

3.4. FOLLOW THE PAST

Follow the Past is a unique path tracking algorithm developed by Dr. Hellström of Umeå University, Sweden. Instead of following a mathematically defined path, it attempts to drive the vehicle along a recorded path, as driven by a human driver. It was also designed for use with a robot for articulated steering, so the output signal corresponds to a steering angle. Like the Stanley Method, the control signal is in the form of the steering angle ϕ

The algorithm determines the steering angle based on three behavior values desired by the controller: ϕ_β , which turns towards the recorded heading, ϕ_γ , which mimics the recorded steering angle, and ϕ_α , which turns towards the desired position along the path. ϕ_β and ϕ_γ are defined trivially:

$$\phi_\beta = \theta' - \theta \quad (19a)$$

$$\phi_\gamma = \phi' \quad (19b)$$

where θ' and ϕ' are the recorded heading and steering angle at the nearest point.

ϕ_α is defined via two methods in Ringdahl and Hellström's paper; the latter will be used here as the original authors state that it is less susceptible to oscillations than the former. In this method, a lookahead point is defined as the sum of a vector with magnitude l in the direction $\theta' + \phi'$, and the path point nearest to the vehicle. ψ is then defined as the heading from the vehicle to the look ahead point. Finally, $\phi_\alpha = \psi - \theta' - \phi'$, such that ϕ_α is the difference in heading from the path point to the look ahead point, and the heading from the vehicle position to the look ahead point. This provides a control value that works to move the vehicle back onto the path, without risking oversaturating the controller if lateral error grows to large, as ϕ_α is inherently bounded between $(-\frac{\pi}{2}, \frac{\pi}{2})$.

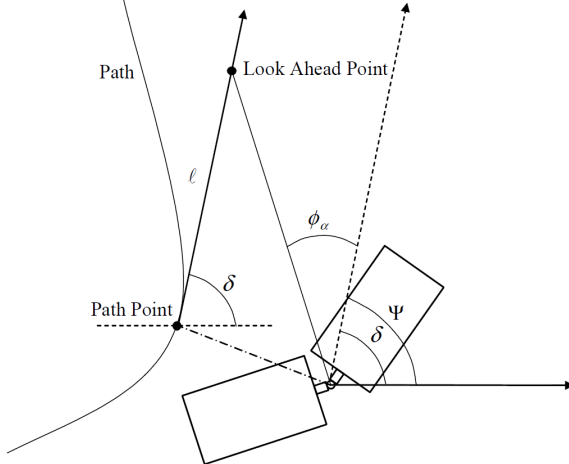


Fig. 4. Geometry of Follow the Past Algorithm from:

(Ringdahl and Hellström 5)

Thereby, the final control law is:

$$\phi = \phi_\alpha + \phi_\beta + \phi_\gamma \quad (20a)$$

which expands to: $\phi = (\psi - \theta' - \phi') + (\theta' - \theta) + \phi'$ (20b)

$$\phi = \psi - \theta \quad (20c)$$

Applying equation 4 yields: $\omega = \frac{v}{l} \tan(\psi - \theta)$ (20d)

3.5. VECTOR PURSUIT

Vector Pursuit is a path tracking method created by Dr. Jeffrey Wit, which describes a desired transformation of the vehicle using Screw Theory, in a similar way to Pure Pursuit's use of arcs. Screws are described by a centerline and a pitch; when combined with an angular movement, it describes the angular and positional transformation on any rigid body. The centerline of such a screw can be defined by a set of Plücker line coordinates. Plücker line coordinates consist of two vectors, $(\vec{S}; \vec{S}_0)$, the first of which is parallel to the center line with unit length, and the second of which is defined as:

$$\vec{S}_0 = \vec{r} \times \vec{S} \quad (21)$$

for any \vec{r} which lies on the center line and \times is the standard cross product. Screw Theory takes this further by adding a pitch component h , and allows the Plücker coordinates to be referred to by a single symbol $\vec{\$}$:

$$\vec{\$} = (\vec{S}; \vec{r} \times \vec{S} + h\vec{S}) = (\vec{S}; \vec{S}_{0h}) \quad (22)$$

The advantage of using this representation is that putting the screw in local coordinates of a rigid body, such that the rigid body is at $(0, 0)$, $\omega \vec{S}_{0h}$ is the instantaneous velocity of the rigid body around the screw. Additionally, if the pitch of the screw tends towards infinity, the screw

models a pure translation in the direction of \vec{S} ; for a velocity v , the screw simplifies to:

$$v\vec{\$} = (\vec{0}; v\vec{S}) \quad (23)$$

as Wit says, it “is a screw that has a centerline at infinity” (44). The intuition for this lies in equation 21; as a zero vector cross a point on the centerline is a finite vector, it follows that every point on the line must have an infinite magnitude.

For the implementation of Vector Pursuit, Dr. Wit considers two methods; however, only the second will be considered for this paper, as it better handles the nonholonomic constraints of the skid-steer testing robot and had better results in Dr. Wit’s own testing. In this implementation, it initially follows similarly to other geometric path tracking methods, in that it selects a goal point that is on the path that is one lookahead distance away from the vehicle. However, unlike those algorithms, Vector Pursuit takes the heading at the goal point into consideration.

The basis of the algorithm is to generate a screw that corrects the translational error, $\vec{\$}_t$, and another screw that corrects the orientation error, $\vec{\$}_r$, and add them together to create a target screw. Each of these screws are defined by the following:

$$\vec{\$}_t = k_t \left(0, 0, 1; {}^W y_v + \frac{d^2}{2 {}^V y_L} \cos \theta_v, -{}^W x_v + \frac{d^2}{2 {}^V y_L} \sin \theta_v, 0 \right) \text{ if } {}^V y_L \neq 0 \quad (24a)$$

$$\vec{\$}_t = k_t \left(0, 0, 0; \frac{{}^W x_L - {}^W x_V}{d}, \frac{{}^W y_L - {}^W y_L}{d}, 0 \right) \text{ if } {}^V y_L = 0 \quad (24b)$$

$$\vec{\$}_r = k_r (0, 0, 1; {}^W y_v, -{}^W x_v, 0) \quad (24c)$$

in which k_t and k_r are gains, d is the lookahead distance, $({}^W x_v, {}^W y_v)$ and θ_v are the position and heading of the vehicle, $({}^W x_L, {}^W y_L)$ is the position of the goal point, and ${}^V y_L$ is the distance from the vehicle to the goal point, only in the vehicle’s lateral direction (Wit 57). When these screws are combined, they yield:

$$\vec{\$}_d = (0, 0, k_t + k_r ;$$

$$k_r {}^W y_v + k_t \left({}^W y_v + \frac{d^2}{2 {}^V y_L} \cos \theta_v \right), -k_r {}^W x_v + k_t \left(-{}^W x_v + \frac{d^2}{2 {}^V y_L} \sin \theta_v \right), 0 \right) \text{ if } {}^V y_L \neq 0 \quad (25a)$$

$$\vec{\$}_d = (0, 0, k_r ;$$

$$k_r {}^W y_v + k_t \left(\frac{{}^W x_L - {}^W x_V}{d} \right), -k_r {}^W x_v + k_t \left(\frac{{}^W y_L - {}^W y_L}{d} \right), 0 \right) \text{ if } {}^V y_L = 0 \quad (25b)$$

After summing the two screws, the gains k_t and k_r are determined by a desired relative proportion k between the amount of time needed to reach the translational target and the amount of time needed to reach the orientation target. For example, if $k = 1$, the algorithm will move the vehicle such that if the motion was sustained, each target would be met at the same time. This allows tuning based on whether position or orientation should be emphasized by the controller.

Upon the substitution of this relationship, the center of $\vec{\$}_d$, $({}^W x_{\vec{\$}_d}, {}^W y_{\vec{\$}_d})$ can be calculated. The distance between the center of the screw and the vehicle is the radius, and from that the curvature of the desired motion can be calculated. These coordinates simplify to:

$${}^W x_{\vec{\$}_d} = {}^W x_v - \frac{k\phi}{(k-1)\phi + (\theta_L - \theta_v)} \left(\frac{d^2}{2 {}^V y_L} \sin \theta_v \right) \quad (26a)$$

$${}^W y_{\vec{\$}_d} = {}^W y_v - \frac{k\phi}{(k-1)\phi + (\theta_L - \theta_v)} \left(\frac{d^2}{2 {}^V y_L} \cos \theta_v \right) \text{ if } {}^V y_L \neq 0, \text{ or} \quad (26b)$$

$${}^W x_{\vec{\$}_d} = {}^W x_v - k \left(\frac{{}^W y_L - {}^W y_v}{\theta_L - \theta_v} \right) \quad (26c)$$

$${}^W y_{\vec{\$}_d} = {}^W y_v - k \left(\frac{{}^W x_L - {}^W x_v}{\theta_L - \theta_v} \right) \text{ if } {}^V y_L = 0 \quad (26d)$$

These variables mean the same as used in previous equations, as well as ϕ being the angle from the vehicle position to the goal point about the screw $\vec{\$}_d$. While Wit uses a more complicated calculation, this angle is most easily calculated from:

$$\phi = 2 \cdot \text{atan2}({}^V y_L, {}^V x_L) \quad (27)$$

This finally is used to calculate the radius of the screw by:

$$r = {}^W y_v \cos \theta_v - {}^W x_v \sin \theta_v - \left({}^W y_{\vec{s}_d} \cos \theta_v - {}^W x_{\vec{s}_d} \sin \theta_v \right) \quad (28a)$$

$$r = \frac{k\phi}{(k-1)\phi + (\theta_L - \theta_v)} \frac{d^2}{2V_{yL}} \text{ if } V_{yL} \neq 0, \text{ or} \quad (28b)$$

$$r = \frac{k}{\theta_L - \theta_v} \left(({}^W y_L - {}^W y_v) \sin \theta_v + ({}^W x_L - {}^W x_v) \cos \theta_v \right) \text{ if } V_{yL} = 0 \quad (28c)$$

Similar to other methods, once the desired radius is found, it can be converted into a desired angular velocity. In this case, ω is:

$$\omega = \frac{v_{current}}{r} \quad (29)$$

Equation 28b includes a $\frac{d^2}{2V_{yL}}$ term, which uses different variables to describe the same principle as Pure Pursuit (equation 12e). However, the inclusion of a coefficient to this allows the tracking algorithm to respond to the desired heading of the path, increasing or decreasing the desired curvature to mitigate overshooting the desired heading. Higher values of k makes this effect more prevalent.

Wit, the original author, claimed that the algorithm “was less sensitive to the chosen look-ahead distance at various speeds [than Pure Pursuit and Follow-the-Carrot], and it was able to handle situations ... after an unexpected obstacle was encountered” (108). Other sources also praise the Vector Pursuit method for its robustness and effectiveness. Lundgren echoes the importance of the property mentioned by Wit, stating that such cases occur in the real world, when a “vehicle detects sudden obstacles appearing on the path,” or “if there is noise in the position estimations, which can happen if the vehicle was using GPS techniques for localizing” (7). While determining the ideal path tracking algorithm for a submersible tracked robot in simulation, Yeu et al. claim that “the tracking performance is better in the vector pursuit than in the pure pursuit” (2785). They attribute this to a slower changing rate of heading angle, which allows for smoother motion of the vehicle.

3.6. RAMSETE

De Luca et al. present a nonlinear control law in their paper "Control of Wheeled Mobile Robots: An Experimental Overview." This nonlinear control law is can be used for any nonholonomic point-to-point motion and is therefore a candidate for a path tracking algorithm. This algorithm will be referred to as Ramsete herein, as that is the acronym for the Italian book in which it was originally published. It considers the most amount of target data for any path tracking algorithm discussed in this paper, considering the desired position (x_d, y_d) , heading θ_d , velocity v_d , and angular velocity ω_d at the goal point. Additionally, contrarily to many other path tracking algorithms, it is nongeometric, having no graphical analogue. Instead, the authors created the control law:

$$v = v_d \cos(\theta_d - \theta) + k_1 [(x_d - x) \cos \theta + (y_d - y) \sin \theta] \quad (30a)$$

$$\omega = \omega_d + k_2 v_d \frac{\sin(\theta_d - \theta)}{\theta_d - \theta} [(y_d - y) \cos \theta - (x_d - x) \sin \theta] + k_3 (\theta_d - \theta) \quad (30b)$$

The authors then prove that the control law is stable for k_i selections of:

$$k_1 = k_3 = 2\zeta \sqrt{\omega_d^2 + bv_d^2}, \quad k_2 = b \quad (30c)$$

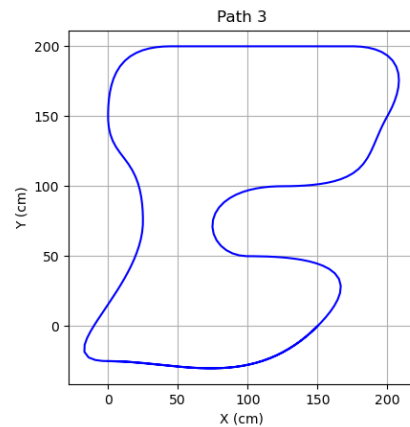
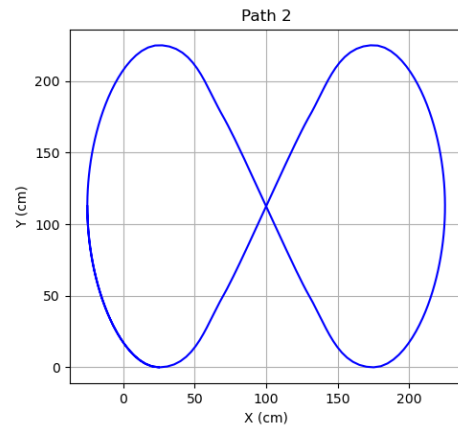
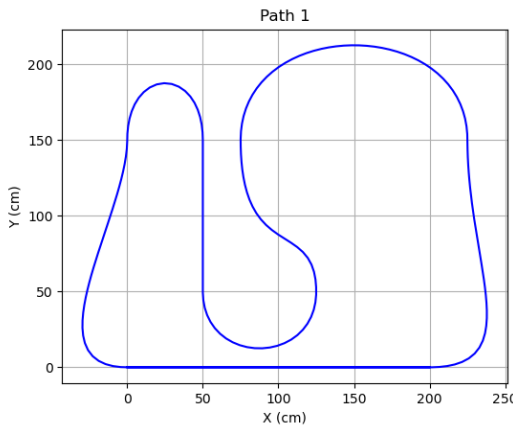
for a gain $\zeta \in (0, 1)$ and a gain $b > 0$. Veness states that ζ acts as a dampening term, for which greater values thereof cause resistance to system change and b acts as a convergence term, for which greater values thereof cause more aggressive convergence to the target (83).

The authors test this control law as a path tracking algorithm in their paper, in which it demonstrates robust tracking. In the primary test of following a figure-eight shaped loop, the average error was 0.5 cm for a robot with dimensions of 46 cm \times 32 cm \times 30.5 cm, showing a very high degree of stability (De Luca et al. 9).

4. TESTING RESULTS

4.1. PATHS AND ERRORS

The following three paths will be used to testing and analysis of the path tracking algorithms. They are chosen to test performance for straight segments, turns, and tight curvatures.



The vehicle's starting position will always be at $(0, 0)$, so for paths 2 and 3 the vehicle must begin its tracking with a corrective maneuver onto the path. As the vehicle will likely not be aligned with the path when it reaches it, it allows for an opportunity to assess how quickly

the vehicle can converge to the path as well as insight as to how quickly any oscillations are damped. However, path 1 may also experience oscillations caused by asymmetric acceleration at the beginning of the path or as a result of error accumulated around a turn.

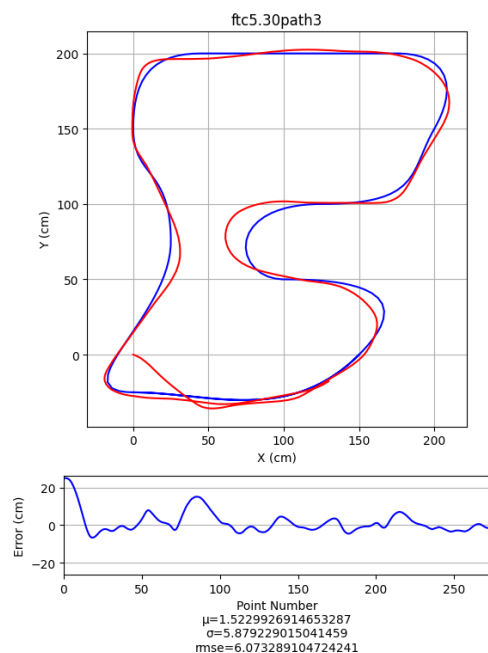
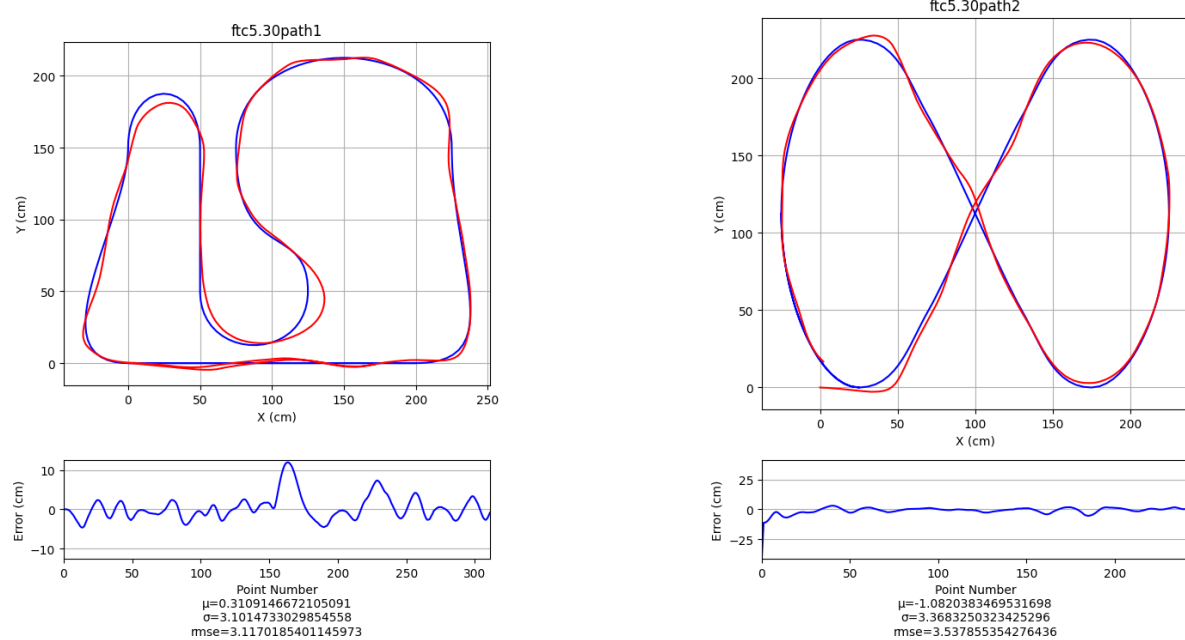
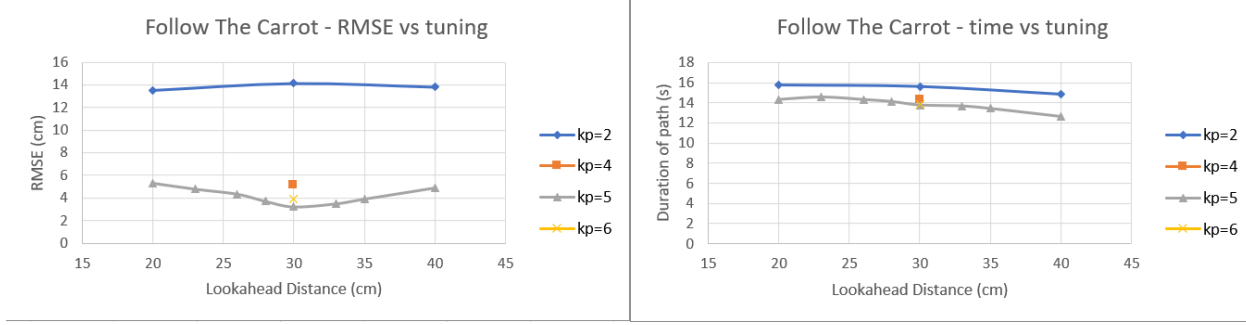
As the paths are arbitrarily parameterized and the vehicle's position function is discontinuous, there are not specific waypoints to which each vehicle point can be ascribed. Therefore error must be determined differently than simply distance formula between pairs of points. Herein, the error function is determined by the minimum distance between each vehicle point and the path for the 14 path segments defined by the 15 waypoints that follow the path segment selected for the previous robot position. For example, the first vehicle point's error is the minimum distance between the vehicle point and the path as defined by the first 15 waypoints. If this minimum distance is determined by the path segment around waypoint P_i , the second vehicle point's error is determined by the path as defined by the waypoints between P_i and P_{i+15} . This ensures that the domain which dictates the error moves with vehicle points, while also correctly ignoring path segments which the vehicle has not yet properly reached, such as the intersection of the figure-8 on path 2. This system will not consider the path's second pass through the intersection while assessing the vehicle's first. Additionally, The sign of the error function is also set by the sign of the cross product between path tangent at P_i and the vector from the path to the vehicle such that errors to the left are positive and errors to the right are negative. This allows for analysis of the vehicle tending towards one side or the other. Error functions are assessed by their mean μ , standard deviation σ , and root mean square error $RMSE$. Performance can also be assessed by the recorded time taken to complete each path, denoted t .

All of the algorithms presented here were tuned such that the standard deviation and root mean square error are minimized on path 1 through trial and error, such that a small increase or decrease in any tuning parameter decreases performance. This tuning was then tested on paths 2

and 3, which gives insight to the algorithm's performance on novel paths.

4.2. FOLLOW THE CARROT

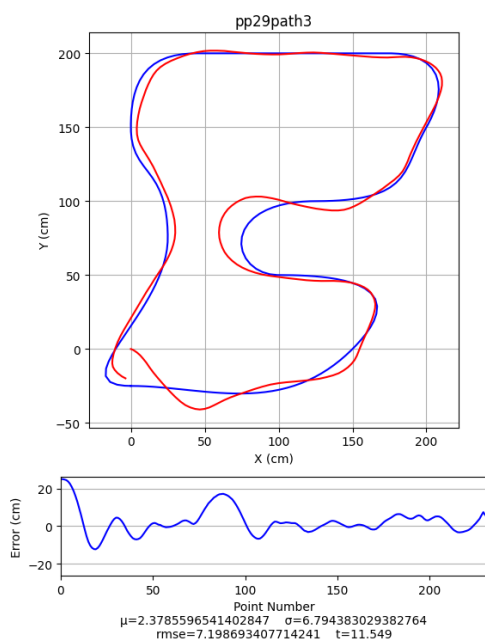
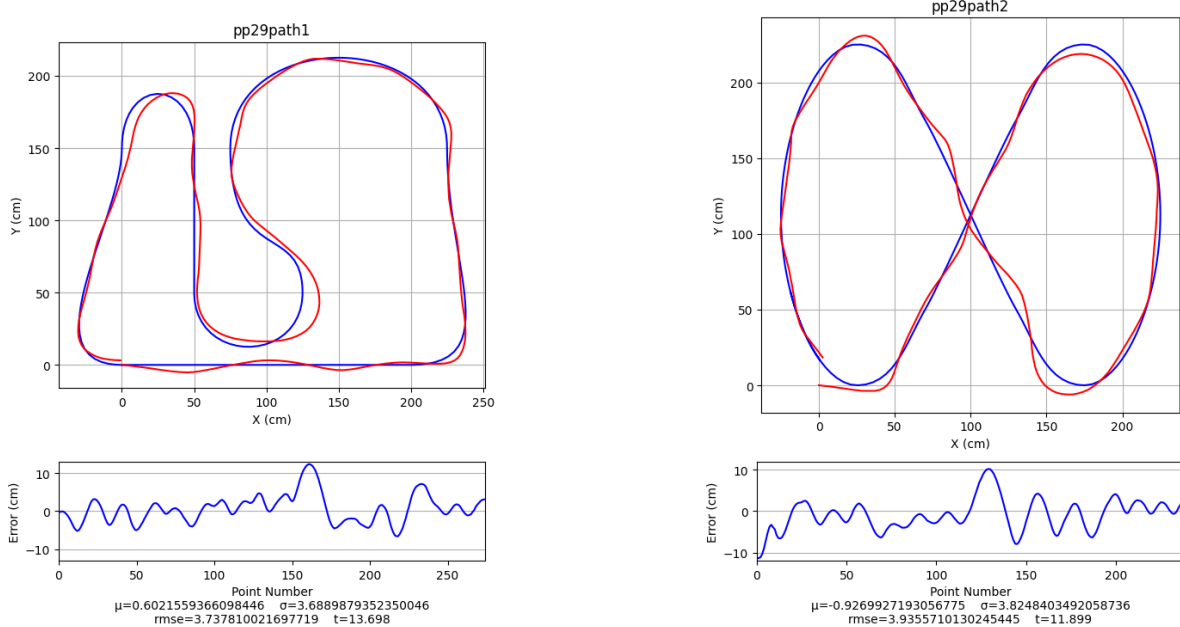
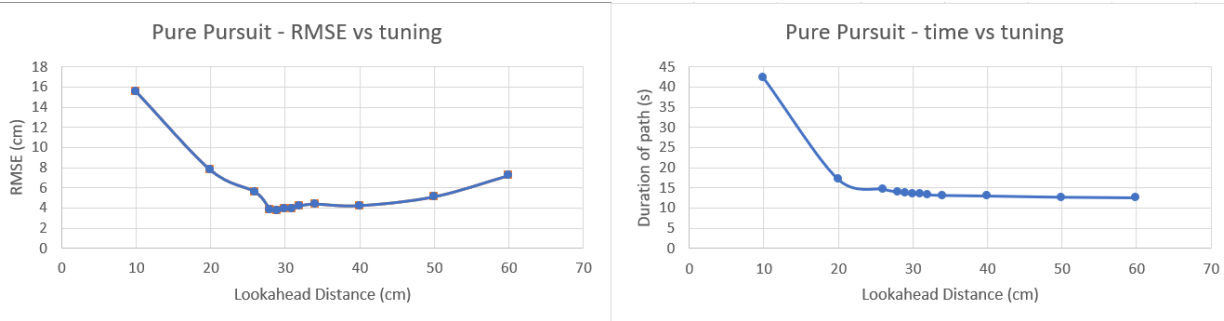
Follow The Carrot greatly exceeded expectations. As expected, the algorithm oscillated over the path; however, the oscillations had a small amplitude that the path was followed fairly accurately, as evidenced by the lowest recorded RMSE on path1. The approximately ideal tuning for this vehicle is $k_p = 5\text{hz}$ and $L = 30\text{cm}$.



The tuning of k_p was reflected in the aggression of the tracking and the frequency of the oscillation. Higher values corresponded to faster oscillation over the path, whereas smaller values tended towards very little oscillation, with the vehicle staying on the outside of each turn. Meanwhile, higher values of L caused the vehicle to tend toward the inside of turns and dampen oscillations. This combination of tuning effects allowed for very good performance of the algorithm.

4.3. PURE PURSUIT

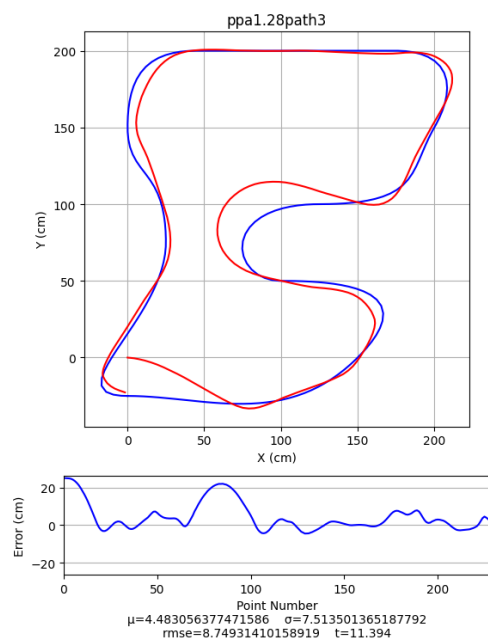
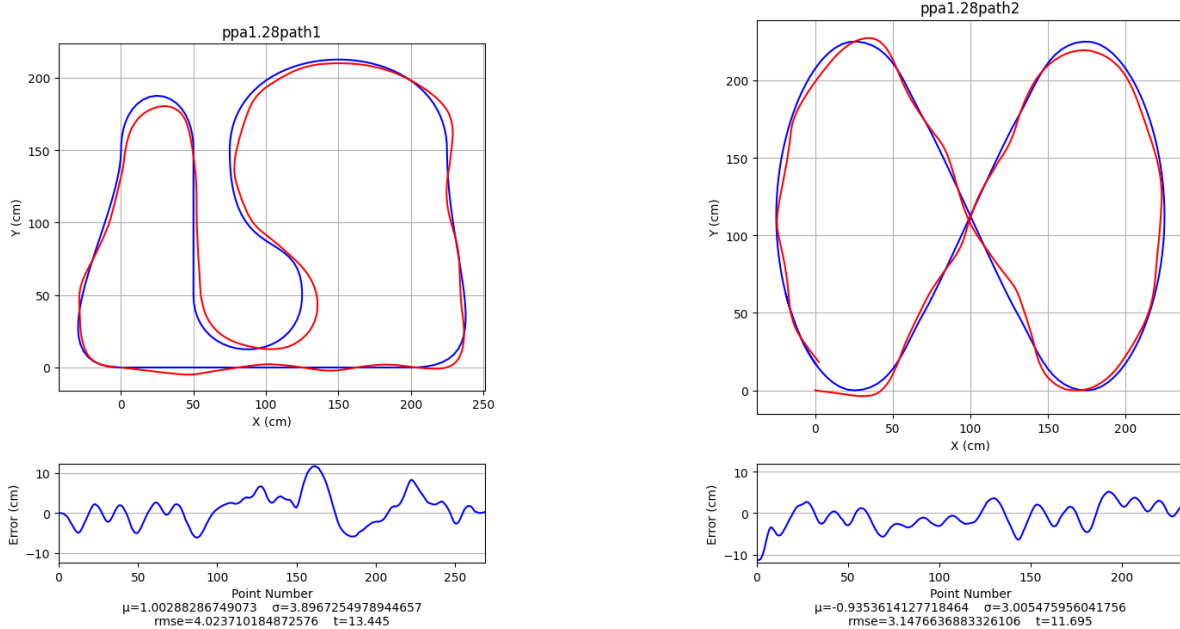
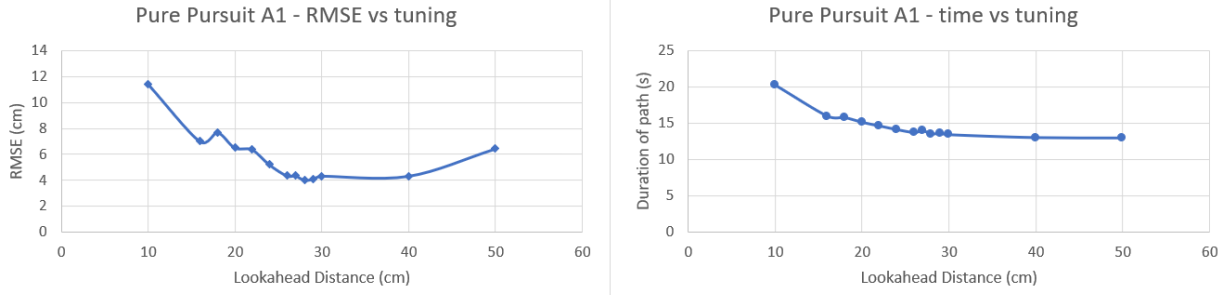
Meeting its expectations as a staple of path tracking algorithm, Pure Pursuit performed well on all three paths. It struggled about tight turns, being unable to follow them well at any tuning. The approximately ideal tuning for this vehicle is $L = 29\text{cm}$.



The tuning of L seemed to be inversely proportional to the aggression of the algorithm. For values less than the ideal, significant oscillations appeared with amplitude and frequency increasing as L decreased. For values greater than the ideal, the oscillations became minimal. However, the vehicle tended to deviate from the path more; namely, the vehicle would move in the outside direction following a turn, while values greater than 40cm would cut inside before a turn, before drifting outside as the turn passed.

4.4. PURE PURSUIT ADAPTIVE - LATERAL ERROR

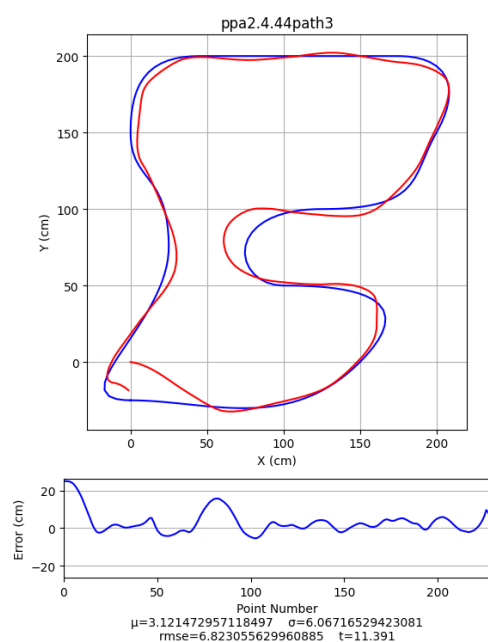
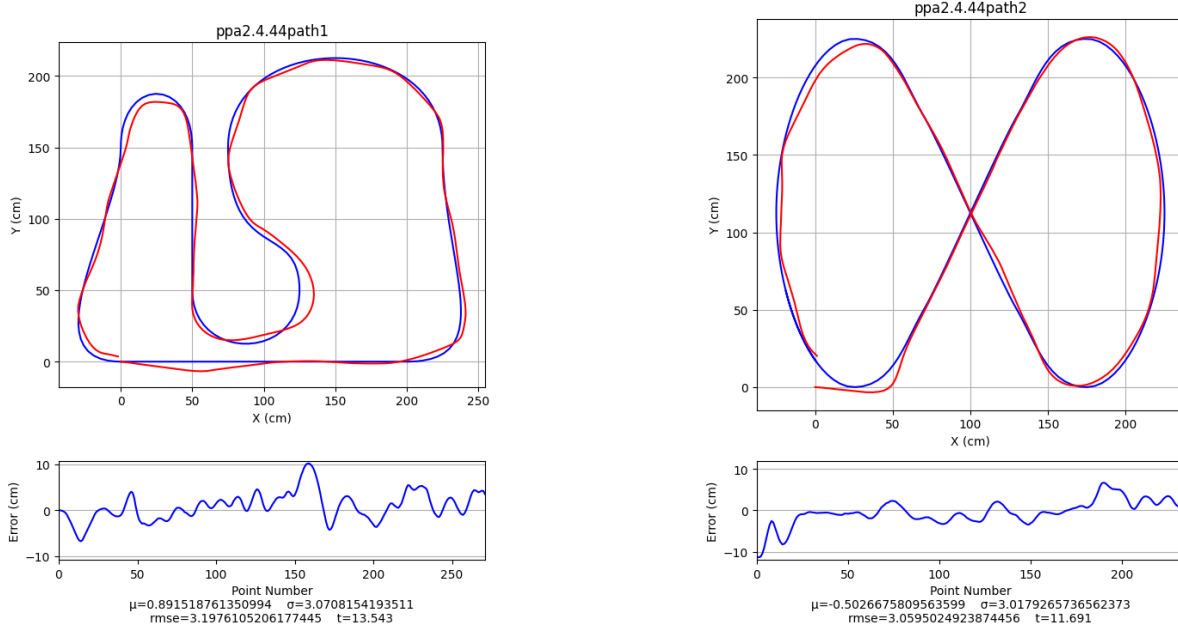
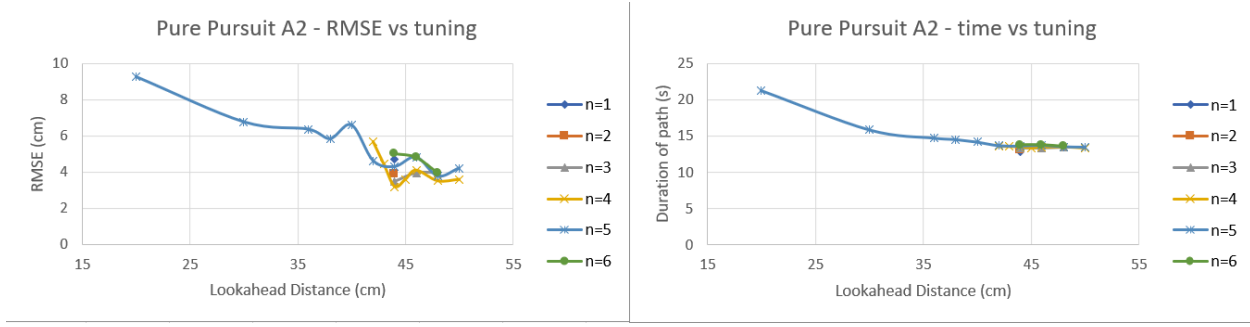
Adapting the lookahead distance by adding the lateral error proved marginally unsuccessful at improving the overall performance of the Pure Pursuit algorithm. As the vehicle strayed from the path, it accumulated lateral error, increasing the lookahead distance, which in turn decreased the algorithm's effort to move back onto the path. As the algorithm sets the effective lookahead distance to a value greater than the base lookahead distance, the approximately ideal tuning for the lookahead distance is decreased slightly to $L = 28\text{cm}$.



This adaptation of Pure Pursuit did not significantly change the effects of changing the lookahead distance. The observations from standard Pure Pursuit hold true for this variant. However, the frequency of the oscillations present at low values of L is decreased, while the effect of tending toward the outside of a turn is increased in higher values of L .

4.5. PURE PURSUIT ADAPTIVE - CURVATURE

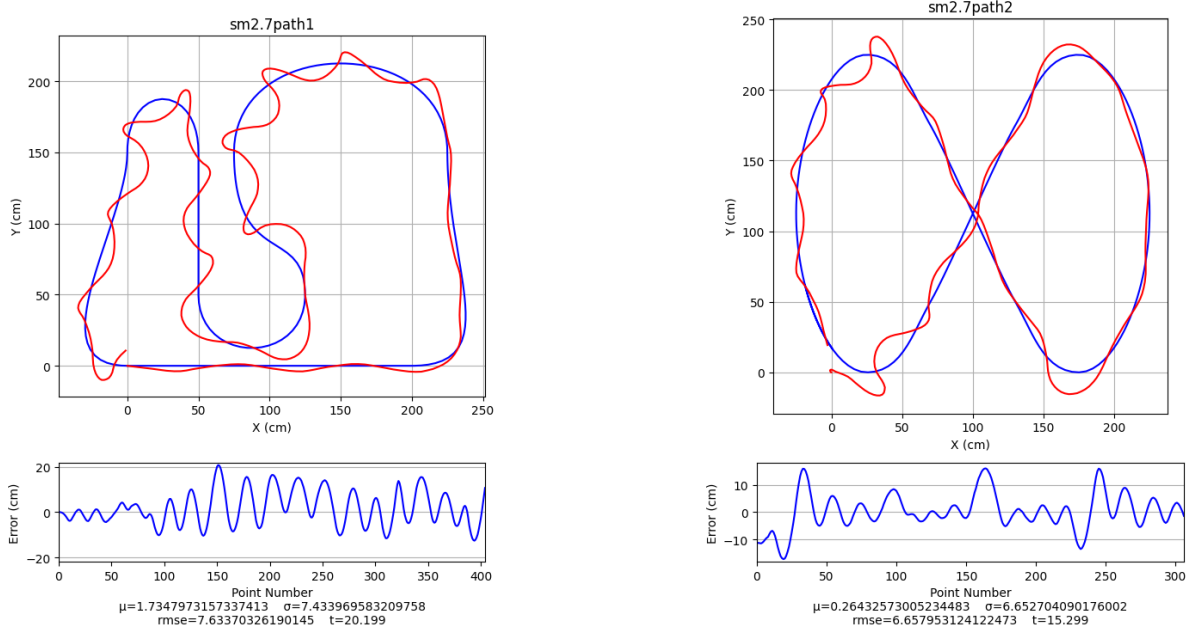
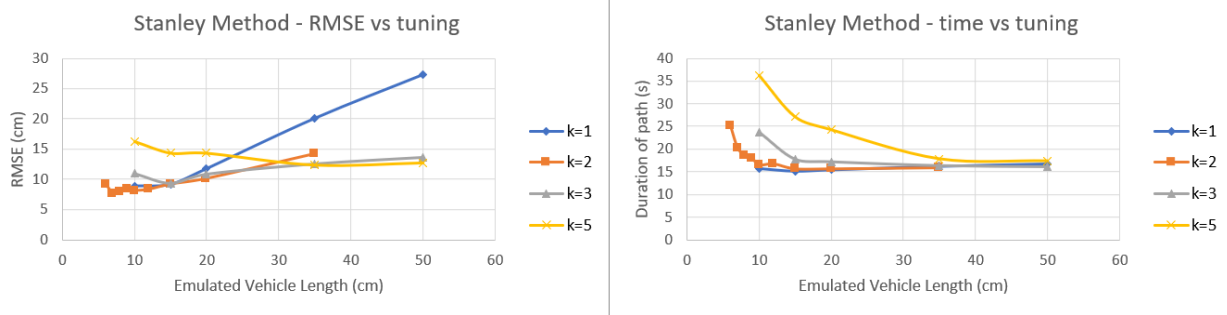
Adapting the lookahead distance by the local curvature proved to be a more successful variation of the Pure Pursuit algorithm than by lateral error and even out-performed the original algorithm in all paths; the reduction of the lookahead distance when approaching an increased curvature pulled the vehicle closer to the path. The approximately ideal tuning for this vehicle is $n = 4$ and $L = 44\text{cm}$.



Unlike the lateral error method of adaptation, this variant of Pure Pursuit had an increased ideal L value as the effective lookahead distance is always smaller than L for this algorithm. This caused severe oscillations for L values as high as 20cm. While this variant had an apparent increase in tracking ability around turns, the vehicle tended to stray from the path after turns. This is likely a result of the local curvature, which only considered the points ahead of the vehicle, dropped to near zero once the turn has passed. A potential improvement to this variation is to sample curvature both ahead and behind of the vehicle in order to maintain a small lookahead distance after a turn. Variation in n had no consistent variation in the algorithm.

4.6. STANLEY METHOD

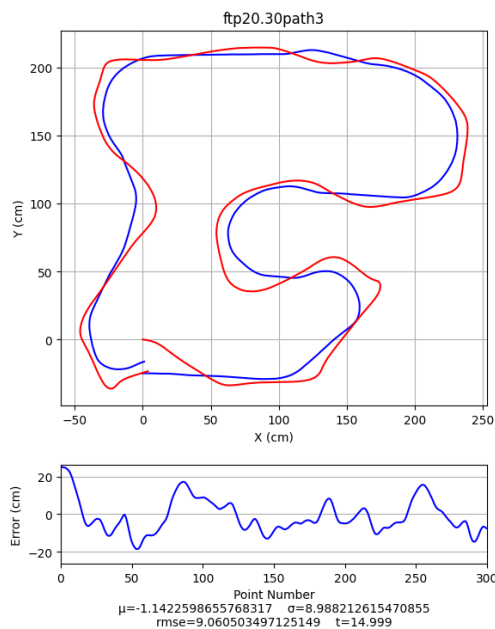
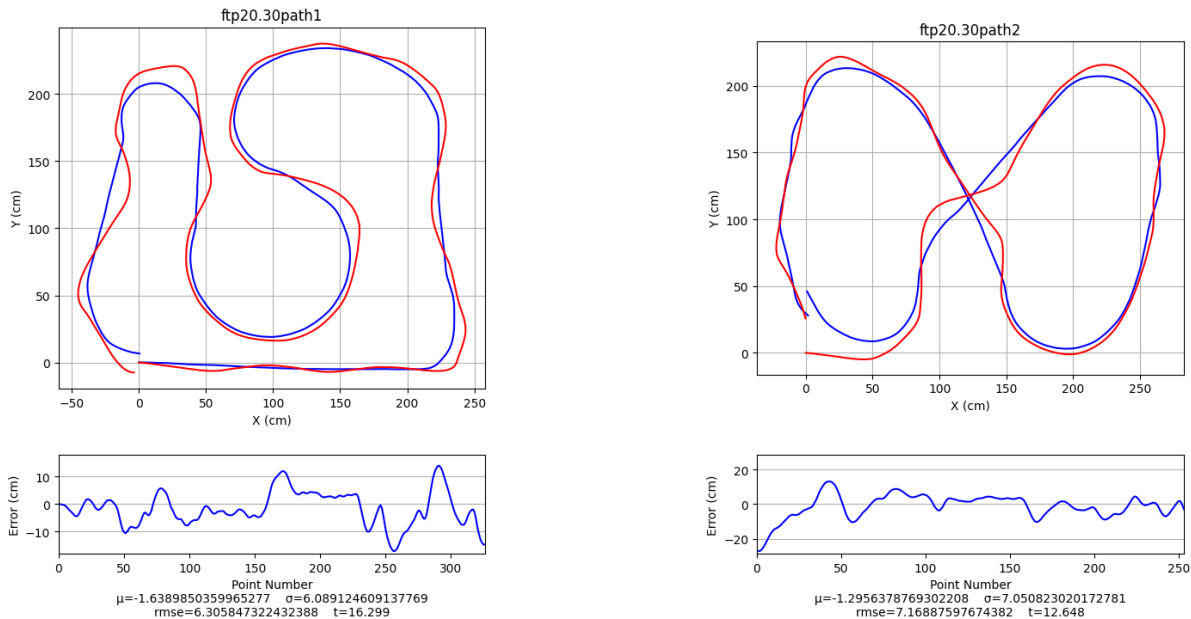
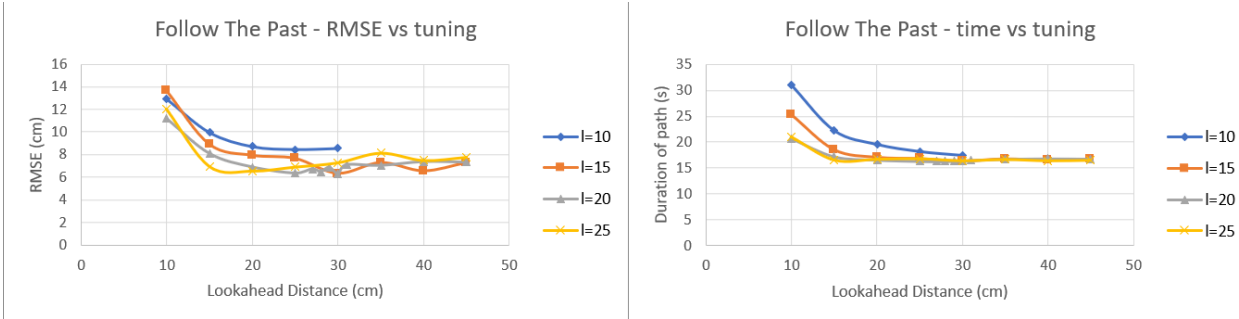
The Stanley Method's trait of only considering the values at the nearest path point seems to decrease the algorithm's ability to track the path tightly around corners. It overshot most turns, tending towards the outside. The approximately ideal tuning for this vehicle is $k = 2\text{hz}$ and $l = 7\text{cm}$.



Values of l larger than 10-15cm, depending on k , trended toward more error as l . k was associated with aggression of the controller, as larger values thereof caused larger and faster oscillations. The vehicle paths created by this algorithm show what appears to be a polygonal shape around turns, with brief segments of turning and relatively long straight segments. This is possibly due to the algorithm's output first going through a tangent function, as control effort increases very quickly when the error inside the tangent function approaches $\frac{\pi}{2}$. This issue may be averted by bounding the domain of the tangent function, simulating a maximum steering angle of an Ackerman-type vehicle. Further research may be required to test this.

4.7. FOLLOW THE PAST

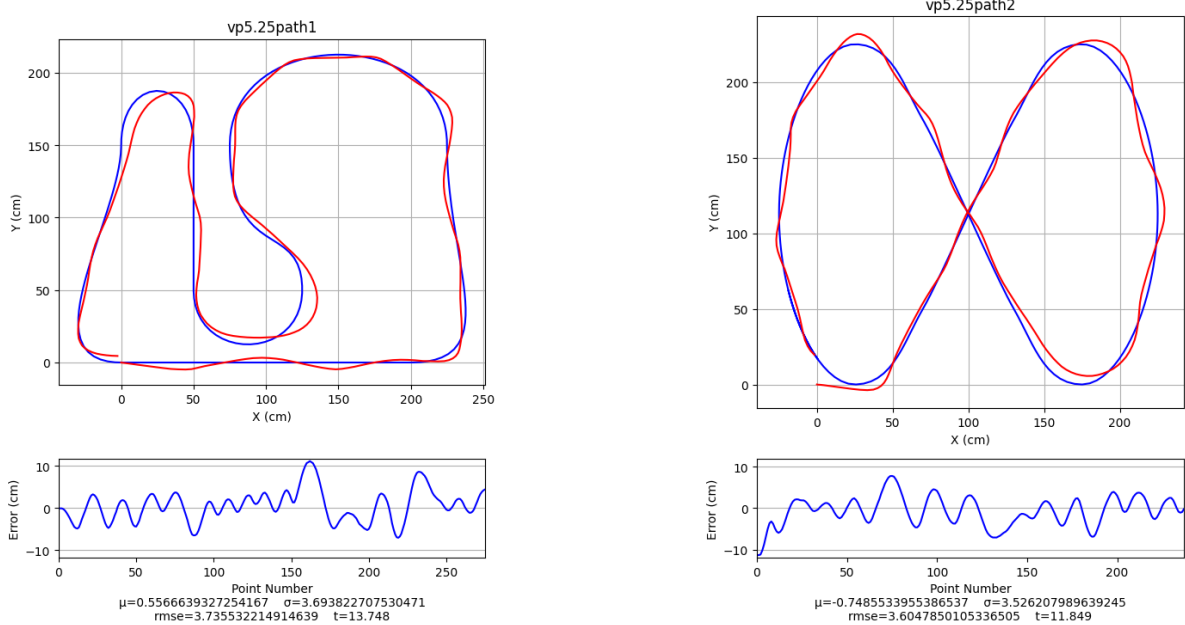
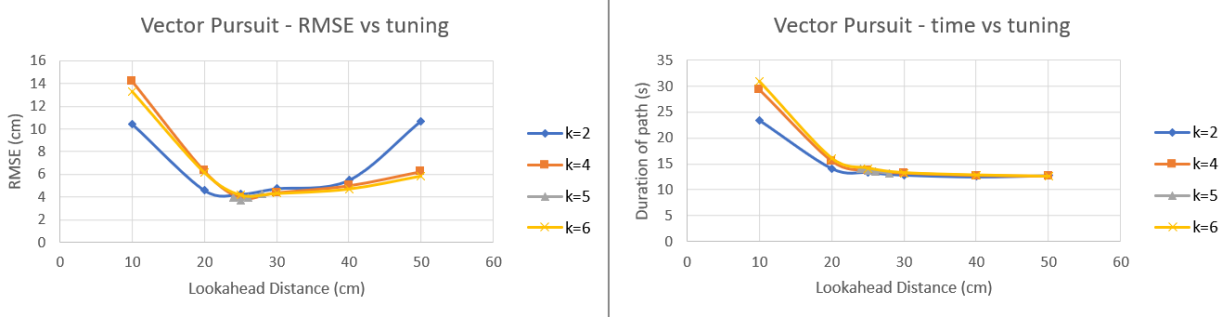
As Follow The Past necessitates a route pre-recorded by a human operator, the standardized paths cannot be used for this algorithm. The standardized paths have been approximately driven, creating equivalent paths for this algorithm. Like the Stanley method, there seems to be an inherent decrease in performance caused by the consideration of the nearest path point as opposed to a lookahead point on the path. Additionally, this algorithm's use of a recorded instead of generated path helps the algorithm by being a definitive path for the vehicle, but also hurts the algorithm by integrating imperfect human control. The approximately ideal tuning for this vehicle is $l = 20\text{cm}$ and $L = 30\text{cm}$.



Lower values of l causes the algorithm to be more aggressive, resulting in higher frequency and amplitude of oscillations, while higher values of l cause more smoothness in the vehicle trajectory. L seems to behave like a dampening term; when small, increasing L makes the path smoother and decreases the amplitude of oscillations. Past the ideal tuning for L , an increase in L allows the vehicle to stray further from the path, particularly on the outside of turns. The same polygonal effect that was seen in the Stanley Method occurs here, and a similar fix may improve the algorithm's effectiveness if applied here.

4.8. VECTOR PURSUIT

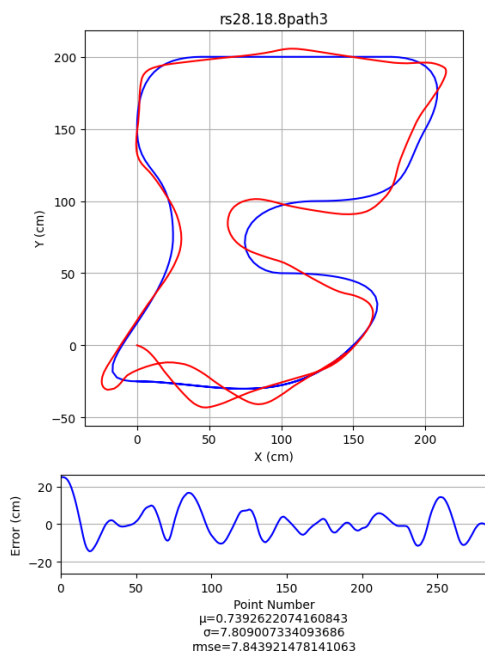
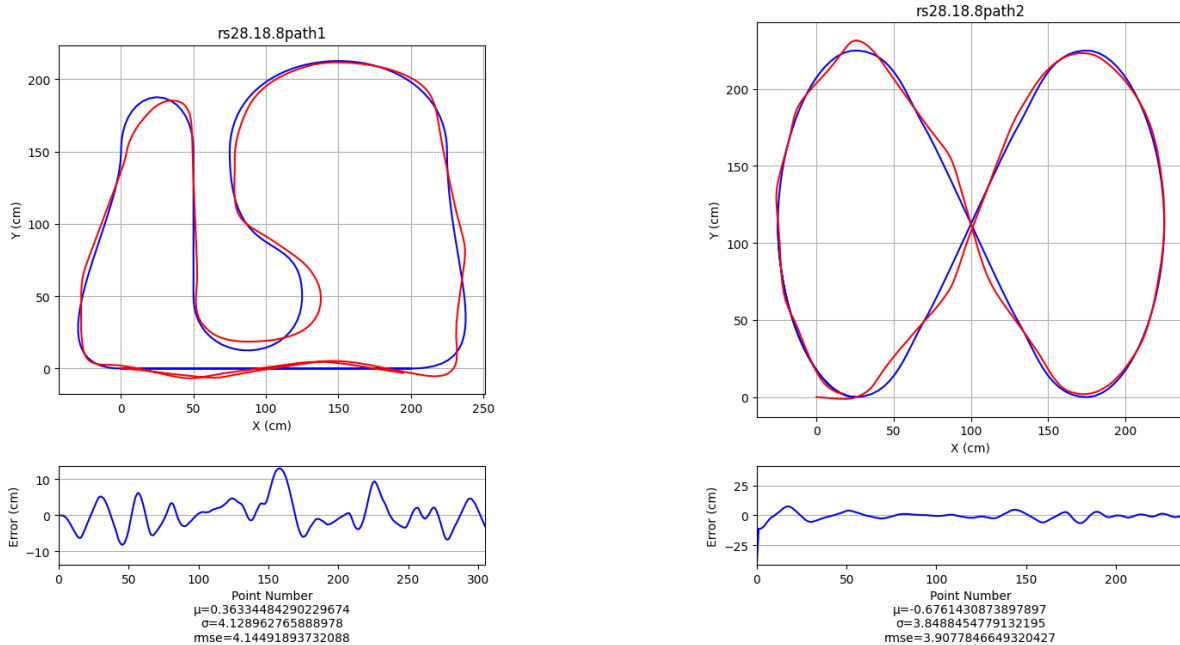
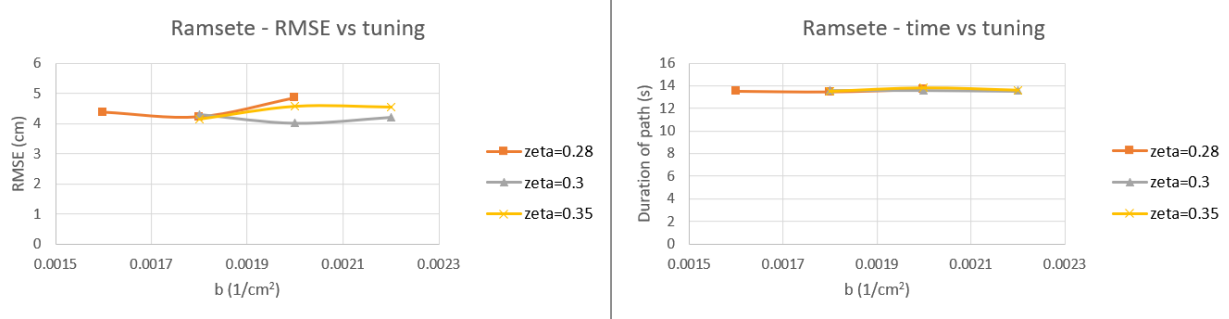
Vector Pursuit, expectedly, performed very similarly to Pure Pursuit. This algorithm's consideration of desired heading on the path seemed to allow it to be slightly more aggressive without unmanageably oscillating, indicated by its better performance at a lower lookahead distance. The approximately ideal tuning for this vehicle is $k = 5$ and $L = 25\text{cm}$.



Tuning of the lookahead distance performed as expected, with higher stability and lower aggression as it increased. Tuning of k revealed generally more aggression for higher values thereof, but not very significantly within the tested domain.

4.9. RAMSETE

Ramsete proved to be robust in its tracking accuracy, getting the very good scores for standard deviation and RMSE on paths 2 and 3. Given that this algorithm was tuned on path 1, the exceptional performance on the other two paths shows that Ramsete is a very consistent algorithm across unique paths. For a lookahead-based tracking algorithm, Ramsete found its tuning with an abnormally low lookahead distance. The approximately ideal tuning for this vehicle is $\zeta = 0.28$, $b = 0.0018\text{cm}^{-2}$, and $L = 8\text{cm}$.



Increasing the ζ term causes a minor increase in the reactivity of the algorithm and draws the vehicle trajectory closer to the inside of turns. Increasing the b term seems to increase the aggression of the algorithm, slightly increasing the amplitude of any oscillations over the path. Finally, increasing the lookahead distance L seems to dampen the oscillations in the system; however, it also allows the vehicle to stray further from the path during sudden turns.

4.10. FURTHER DATA

While the tunings that minimize error are displayed above, there are many more values that were tested and analyzed in the pursuit of these approximately ideal tunings. All of the data and additional graphs and images related to this project are available [here](#).

5. CONCLUSION

The growing development in self-driving cars and other autonomous vehicles has made path tracking and its ability to control a nonholonomic vehicle's movement through a plane a significant field for robotics. This paper describes a number of path tracking algorithms, as well as an implementation of path planning, odometry, and motor control: the other functions required for path tracking. The testing of these path tracking algorithms here indicates that Follow The Carrot is the best performing algorithm on this test vehicle. However, the data also indicates possible improvements in the algorithms in order to produce higher accuracy and lower error, such as different domains of path sampling and bounded control output. Further research is required to see how these improvements will perform.